

## **UC Davis**

### **UC Davis Previously Published Works**

**Title**

Alkaline Cellulose Nanofibrils from Streamlined Alkali Treated Rice Straw

**Permalink**

<https://escholarship.org/uc/item/3jd625dh>

**Journal**

ACS Sustainable Chemistry & Engineering, 5(2)

**ISSN**

2168-0485

**Authors**

Gu, Jin

Hsieh, You-Lo

**Publication Date**

2017-02-06

**DOI**

10.1021/acssuschemeng.6b02495

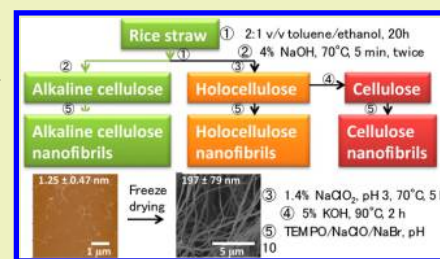
Peer reviewed

## Alkaline Cellulose Nanofibrils from Streamlined Alkali Treated Rice Straw

Jin Gu<sup>†,‡</sup> and You-Lo Hsieh<sup>\*,‡</sup><sup>†</sup>College of Materials and Energy, South China Agricultural University, Guangzhou, Guangdong 510642, China<sup>‡</sup>Fiber and Polymer Science, University of California, Davis, California 95616, United States

**ABSTRACT:** Alkali treatment (4% NaOH, 70 °C, 5 min, twice) of dewaxed rice straw was effective in removing most hemicelluloses, lignin and silica to yield 47.6% cellulose-rich solid. Optimal TEMPO oxidation (7.5 mmol NaClO per gram of alkaline cellulose) followed by mechanical defibrillation (30 min) produced 36.5% alkaline cellulose nanofibrils (ACNFs), higher than the 29.1% CNFs from sodium chlorite oxidation-alkali leaching as well as the 33.7% HCNFs from sodium chlorite oxidation. At the same 5 mmol NaClO level, ACNFs were similar in lateral dimensions ( $1.25 \pm 0.47$  nm) and crystallinity (68%), but less surface oxidized (65%) than CNFs and HCNFs ( $1.55 \pm 0.54$  and  $1.36 \pm 0.62$  nm, 69% and 68% CrI, 85% and 69% surface oxidization, respectively). While the residual noncellulosics consumed oxidizing agents, their presence led to longer ACNFs and HCNFs, higher thermal stability, and thinner self-assembling fibers (197 and 94 nm, respectively) than CNFs (497 nm). Therefore, this facile alkali pretreatment is not only highly efficient in preparing ACNFs with attributes similar to CNFs and HCNFs, but like HCNFs due to their less pristine nature, also present some unique properties that are promising for advanced applications.

**KEYWORDS:** Cellulose nanofibrils, TEMPO oxidation, Alkali treatment, Rice straw, Self-assembly



## INTRODUCTION

Biobased materials and fuels generated from agricultural crop residues valorize nonedible lignocellulose fractions while also reducing their impact on the environment. Crop residues consist mainly of cellulose, hemicelluloses, and lignin, and their exact chemical compositions depend on the origin and methods of extraction. In recent decades, nanocelluloses have attracted increasing interest due to their exceptional mechanical, thermal, and biological properties.<sup>1,2</sup> In addition to those most studied from wood pulp, nanocelluloses have been increasingly reported from agricultural residues, such as crop stalks, straws, bagasses, and husks<sup>3</sup> including rice straw and husk.

Nanocelluloses have been typically prepared from cellulose isolated from the biomass by alkali and/or acid treatments together with bleaching. Soda pulping is a classic method to obtain cellulosic pulps from crop straws<sup>4</sup> in that sodium hydroxide breaks the  $\alpha$ -ether linkages and ester bonds between lignin and/or hemicelluloses to dissolve and remove the noncellulosic components.<sup>5,6</sup> In the case of nonwood plants, bleaching is not as essential since the starting materials generally contain less lignin than woody plants.<sup>7</sup> Also, alkali dissolved hemicelluloses and lignin have found potential applications as food additives, biodegradable films, biofuel productions, and/or carbon fibers.<sup>8–12</sup> Therefore, alkali treatment alone has the promise of isolating cellulose-rich components from lignocelluloses while exerting less impact on the environment.

Rice straw, the most abundant agricultural byproduct in the world, was reported to contain 28–36% cellulose, 23–28% hemicelluloses, 12–14% lignin, and 14–20% silica ash.<sup>13</sup>

Various rice straw nanocelluloses have been produced, including cellulose nanocrystals by sulfuric acid hydrolysis<sup>14–16</sup> and cellulose nanofibrils (CNFs) by TEMPO (2,2,6,6-tetramethylpiperidine-1-oxyl)-mediated oxidation combined with mechanical means using a homogenizer or blender<sup>16–19</sup> or by mechanical means only, such as sonication<sup>20</sup> and collision of pressurized aqueous jets.<sup>21</sup>

Cellulose has been isolated from rice straw by stepwise processes to remove each of the noncelluloses, i.e., toluene/ethanol dewaxing, acid hydrolysis and/or alkaline leaching of hemicelluloses, and sodium chloride bleaching of lignin.<sup>14,20</sup> Coupling TEMPO oxidation with mechanical blending has shown to increase the yield of CNF from this purified rice straw cellulose to a far superior 96.8%.<sup>18</sup> When the same coupled TEMPO oxidation and mechanical blending was applied to holocellulose derived by omitting the second alkaline leaching step, most remaining noncellulosic components including hemicelluloses and/or lignin were degraded to water-soluble fractions by the oxidizing agents.<sup>17</sup>

This study was to investigate further streamlining the isolation process by eliminating the sodium chlorite bleaching step from our previously reported three-step process<sup>14</sup> and the properties of CNFs so produced in comparison to those from the most purified cellulose<sup>18</sup> and holocellulose.<sup>17</sup> The streamline process involved optimizing alkaline pretreatments of toluene/ethanol (2:1) extracted rice straw by studying the

Received: October 14, 2016

Revised: November 23, 2016

Published: December 27, 2016

effect of NaOH concentrations (4, 6, and 8 w/v%) and time (5 min to up to 120 min) at 70 °C as well as repetition of the optimal condition. The optimally alkali treated rice straw cellulose was then subjected to TEMPO oxidation at three primary oxidant levels of 5, 7.5, and 10 mmol NaClO per gram of cellulose at pH 10 followed by mechanical blending to find the optimal TEMPO condition for the highest yield. The morphology, yield, chemical composition, self-assembled structure, crystal structure, and thermal stability of the resulting alkali treated cellulose nanofibrils (ACNFs) were analyzed and compared with two other rice straw nanocelluloses, i.e., CNFs from cellulose derived from the sodium chlorite-alkaline extraction process,<sup>18</sup> and HCNFs from holocellulose derived from the sodium chlorite oxidation process.<sup>17</sup> The endeavor is to offer cellulose nanofibrils from yet another cellulose precursor isolated by a less demanding and streamlined alkaline pulping pretreatment.

## ■ EXPERIMENTAL SECTION

**Materials.** Rice straw (Calrose variety) was harvested in the Sacramento valley in 2009. Toluene (certified ACS, Fisher Scientific), ethanol (anhydrous, histological grade, Fisher Scientific), sodium hydroxide (NaOH, 1 N, Certified, Fisher Scientific), sodium hypochlorite (NaClO, 10.6%, reagent grade, Sigma-Aldrich), 2,2,6,6-tetramethylpiperidine-1-oxyl (TEMPO, 99.9%, Sigma-Aldrich), sodium bromide (NaBr, BioXtra, 99.6%, Sigma-Aldrich), and hydrochloric acid (HCl, 1 N, Certified, Fisher Scientific) were used as received. Water was purified using a Milli-Q plus water purification system (Millipore Corporate, Billerica, MA) in all experiments.

### Isolation of Cellulose from Rice Straw by Alkali Treatment.

Washed and dried rice straw (30 g) was milled to fine powder (60 mesh, Thomas-Wiley Laboratory Mill model 4, Thomas Scientific), oven-dried (50 °C, 48 h), and extracted with the toluene/ethanol (2:1, v/v, 450 mL) mixture for 20 h to remove wax, pigments, and oils. The dewaxed rice straw was treated with 4%, 6%, and 8% (w/v) of NaOH at 70 °C for 5 min to up to 120 min to find the optimal conditions to extract cellulose. The insoluble part was separated by centrifugation (5000 rpm, 15 min), and the precipitate was washed with DI water until pH reached neutral, frozen in liquid nitrogen (−196 °C), and lyophilized at −50 °C in a freeze-drier (FreeZone 1.0 L Benchtop Freeze-Dry System, Labconco, Kansas City, MO). The alkali treated celluloses (ACs) were designated as AC8-120, AC6-120, AC4-120, AC4-5-5, etc., with the first number indicating w/v percent of aqueous NaOH, with the second number being minutes in treatment time and the third the number being repetition in treatment, if any.

For comparison, rice straw holocellulose and cellulose were also prepared according to a previously reported method.<sup>14</sup> Briefly, the dewaxed rice straw was oxidized with 1.4% acidified NaClO<sub>2</sub> at 70 °C for 5 h to remove lignin and obtain holocellulose. The initial pH of the solution was adjusted to 3.0–4.0 by CH<sub>3</sub>COOH. Rice straw cellulose was obtained by treating the holocellulose powder with 5% KOH at room temperature for 24 h and then at 90 °C for 2 h.

**Isolation of Cellulose Nanofibrils from Alkali Treated Rice Straw.** AC4-5-5 was used to produce cellulose nanofibrils (ACNFs) using TEMPO-mediated oxidation followed by mechanical defibrillation as reported previously.<sup>18</sup> Generally, 1 g of freeze-dried AC4-5-5, 0.016 g of TEMPO, and 0.1 g of NaBr were added to 100 mL of DI water. Oxidation reaction was initiated by adding NaClO of three different levels, 5, 7.5, and 10 mmol per gram of AC, respectively, and conducted at 9.8–10.2 pH adjusted by adding 0.5 M NaOH. The reaction lasted until there was no further decrease in pH, and the length of reaction time was recorded. The suspension was neutralized to pH 7 with 0.5 M HCl, centrifuged (5000 rpm, 15 min), and dialyzed against DI water to obtain TEMPO-oxidized AC (i.e., TAC5, TAC7.5, and TAC10 where the number indicated the NaClO concentration). These products were then mechanically defibrillated using a household blender (30 min, 37 000 rpm) and centrifuged again (5000 rpm, 15 min) to obtain nanofibril containing supernatants. The

products were named alkali treated cellulose nanofibrils (i.e., ACNF5, ACNF7.5, and ACNF10). All yields were based on the mass of the original rice straw unless specified.

For comparison, rice straw holocellulose and cellulose purified with the NaClO<sub>2</sub> oxidation step were also TEMPO-oxidized using 5 mmol of NaClO as initiator to obtain TEMPO-oxidized holocellulose (THC5) and cellulose (TC5) followed by the same mechanical defibrillation procedure to obtain HCNF5 and CNF5 as reported previously.<sup>17</sup>

**Self-Assembly of Fibrous Cellulosic Materials.** ACNF aqueous suspension of 0.1 wt % (5 mL) was placed in a 15 mL centrifuge tube, quickly immersed into liquid nitrogen (−196 °C), and lyophilized at −50 °C in the freeze-drier. The ACNFs were thus self-assembled into submicron fibers.

**Analysis.** The chemical structure of the ACs was analyzed by Fourier transform infrared spectroscopy (FTIR) (Nicolet 6700, Thermo Scientific). The FTIR samples were prepared by mixing freeze-dried ACs with KBr at 1:100, w/w CNF:KBr ratio. The FTIR spectra were obtained from 64 scans over 4000–400 cm<sup>−1</sup> at a resolution of 4 cm<sup>−1</sup> under transmission mode.

Neutral sugar composition, Klason-lignin content, and ash content of dewaxed rice straw, AC4-5-5, holocellulose, cellulose, TAC5, THC5, and TC5 were determined according to standard procedures (Sluiter et al. 2005 and Sluiter et al. 2008). After sulfuric acid hydrolysis, the neutral sugar composition analysis was carried out using a high-performance anion-exchange chromatography with pulsed amperometric detection (HPAEC-PAD, Dionex, ICS-3000).

The morphology of individual ACNFs was studied by atomic force microscopy (AFM, Asylum-Research MFP-3D). ACNF suspensions of 10 μL (0.0005 wt %) were deposited onto freshly cleaved mica surfaces and air-dried. The samples were scanned under ambient conditions using tapping mode with OMCL-AC160TS standard silicon probes. The scan rate was set to 1 Hz. The height images and profiles were processed with Igor Pro 6.21 software, and 100 samples were used to calculate the averaged thickness of ACNFs.

The total surface carboxylate/carboxylic (COO<sup>−</sup>/COOH) content of the ACNFs was measured by conductometric titration. A certain amount of 1 N HCl was added to the ACNF suspension (50 mL, 0.1 wt %) to protonate the carboxyl group, and the suspension was titrated with 0.02 M NaOH solution. The changes of the suspension conductivity values were recorded by an OAKTON pH/Con 510 series meter. The total COOH and COO<sup>−</sup> contents (σ<sub>COOH+COO<sup>−</sup></sub>, in mmol per gram of cellulose nanofibrils) were determined as follows:

$$\sigma_{\text{COOH}+\text{COO}^-} = \frac{cv}{m} = \frac{c(v_2 - v_1)}{m} \quad (1)$$

Here  $c$  is the NaOH concentration (0.02 M),  $m$  is the mass of the suspension (0.050 g), and  $v_1$  and  $v_2$  are NaOH volumes (in mL) used for neutralizing the added HCl and carboxylic acid groups, respectively. The total  $\sigma_{\text{COOH} + \text{COO}^-}$  (in mmol per gram of cellulose nanofibrils) was also converted to total COOH and COO<sup>−</sup> content (in mol per mol of anhydroglucose (MW: 162 g/mol)) or glucuronic acid (MW: 176 g/mol) weight percent (in grams per gram of cellulose nanofibrils).

The self-assembled structure of the freeze-dried ACNFs was analyzed by a field emission scanning electron microscope (FE-SEM) (Merlin, Zeiss, Germany). The sample was mounted on conductive carbon tape and sputter coated with gold. The SEM was operated at 5 mm working distance and 5 kV accelerating voltage. The silicon concentration of the samples was evaluated by energy-dispersive X-ray spectroscopy (EDS) adjacent to the SEM. The average diameters of self-assembled fibers were obtained from more than 100 individual fibers by image software (ImageJ, NIH, USA).

The crystal structure of the ACNFs was analyzed by X-ray diffraction (XRD, Scintag XDS 2000 powder diffractometer). Diffractograms of the freeze-dried ACNFs were collected with Ni filtered Cu K $\alpha$  radiation generated at 45 kV and 40 mA at a rate of 2 deg/min from 5° to 40° 2 $\theta$ . The crystallinity (CrI), crystallite sizes, primary C6 hydroxyl groups, and primary hydroxyl-to-carboxyl

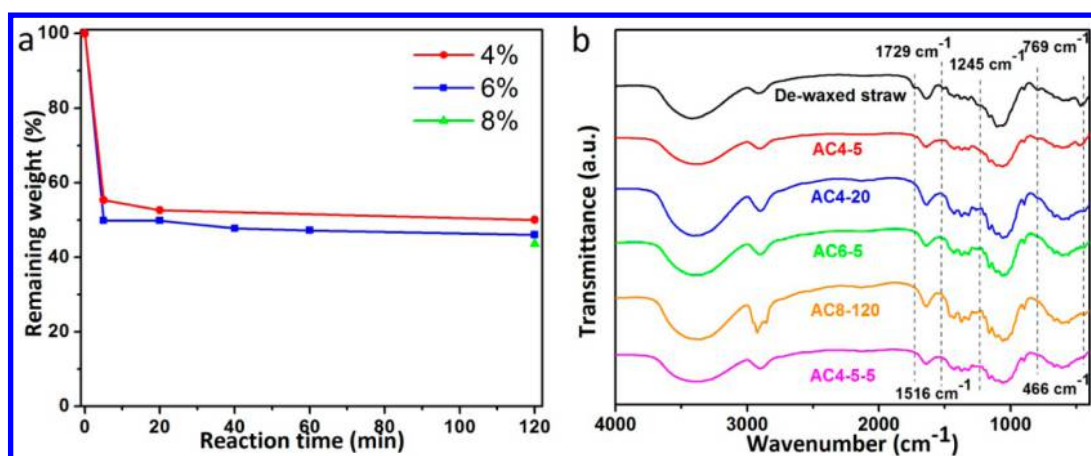


**Figure 1.** Alkali treated celluloses (ACs): (a) yields at different NaOH concentrations and times; and (b) FTIR spectra of dewaxed rice straw and ACs, where the first number indicates NaOH concentration in %, the second number denotes treatment time in min, and the third (if any) indicates repeating treatment time in min.

**Table 1. Nanocellulose Generated from Coupled TEMPO Oxidation<sup>a</sup> and Blending of Cellulose Isolated by Different Processes**

isolation		TEMPO oxidation			nanofibril			COOH + COO <sup>-</sup> content (mmol/g)
starting ligno-cellulose	yield <sup>b</sup> (%)	TEMPO oxidation <sup>a</sup>	reaction time (min)	yield <sup>b</sup> (%)	blending	yield <sup>b</sup> (%)	thickness (nm)	
AC4-5-5	47.6	TAC5	30	39.7	ACNF5	34.2	1.25 ± 0.47	0.96
		TAC7.5	79	38.3	ACNF7.5	36.5	1.36 ± 0.83	1.25
		TAC10	168	31.5	ACNF10	30.2	1.40 ± 0.76	1.62
cellulose	35.5	TCS	71	30.8	CNF5	29.1	1.55 ± 0.54	1.36
holocellulose	72.8	THCS	86	37.9	HCNF5	33.7	1.36 ± 0.62	1.09

<sup>a</sup>Number denotes NaClO concentration in mmol per gram of starting lignocellulose. <sup>b</sup>All yields are based on original rice straw mass. The data on cellulose,<sup>17,18</sup> holocellulose,<sup>17</sup> and their respective derivatives are taken from our previous studies.

conversion percent on cellulose crystal surfaces were determined following a previous study.<sup>18</sup>

The thermal properties of the ACNFs were analyzed with a thermogravimetric analyzer (TGA-50, Shimadzu). Freeze-dried ACNF sample of roughly 5 mg was weighed and heated from ambient to 500 °C at a rate of 10 °C per min under N<sub>2</sub> atmosphere (50 mL/min).

## RESULTS AND DISCUSSION

**Optimization of Alkali Treatment.** Organic extraction of cleaned and dried rice straw powder in 2:1 toluene/ethanol yielded 94.4% dewaxed rice straw that was then treated with 4%, 6%, and 8% (w/v) NaOH at 70 °C for up to 120 min. The most significant mass losses of 44.7% and 50.2% were observed after treatment for 5 min with 4% and 6% NaOH, respectively, losing slightly more to a total of 50.0–56.5% with 8% NaOH up to 120 min (Figure 1a). The brown color of rice straw was reduced with increasing concentrations and times, but a light yellow color remained, indicating the presence of lignin in the alkali treated rice straw cellulose even under the most extensive alkali treatment conditions. The alkaline cellulose yield was 52.2%, 47.0%, and 41.1% of original rice straw for AC4-5, AC6-5, and AC8-120, respectively, showing most noncelluloses in the rice straw to be readily dissolved in 4% NaOH within 5 min, while leaving some residual lignin.

The FTIR spectra of dewaxed rice straw showed an aromatic skeletal vibration at 1516 cm<sup>-1</sup>, characteristic of lignin, as well as hemicellulose carboxyl C=O stretching at 1729 cm<sup>-1</sup> and C—O stretching at 1245 cm<sup>-1</sup>, with the latter indicative of xylan,<sup>22</sup> a major hemicellulose in rice straw (Figure 1b). The hemicellulose C=O stretching at 1729 cm<sup>-1</sup> disappeared in all AC samples while the xylan C—O stretching at 1245 cm<sup>-1</sup> was

only found in AC4-5, indicating easy dissolution of hemicelluloses with 4% NaOH and eventual xylan removal at above 4% NaOH, all within 5 min. While all AC samples were a slight light yellow color indicative of the presence of lignin, the lignin quantities in them were too low to be detected by FTIR. The 796 and 466 cm<sup>-1</sup> bands in dewaxed rice straw attributed to Si—O—Si stretching<sup>14</sup> decreased with increased NaOH concentrations and times, but remained observable in all cases. The presence of the silica peaks in AC8-120 indicated silica to be only partially soluble even in 8% NaOH. These above data showed that nearly all hemicelluloses and lignin in the rice straw could be easily dissolved in 4% NaOH in 5 min, but not silica.

The optimal alkali treatment (4% NaOH, 5 min) was repeated a second time to lower the mass by another 4.6% to yield 47.6% AC4-5-5 whose FTIR showed neither silica nor hemicellulose bands (Figure 1b). Within the detection limit of FTIR, this repeated alkali treatment appeared to be effective in removing most of the noncellulosic materials in rice straw. The AC4-5-5 yield was 12.1% higher than the 35.5% pure cellulose by a three-step dewaxing–sodium chlorite oxidation–alkaline leaching process reported earlier.<sup>14</sup>

**TEMPO Oxidation of Alkali Treated Rice Straw Cellulose to Nanofibrils.** The optimally alkali treated cellulose AC4-5-5 was TEMPO-oxidized at three primary oxidant levels of 5, 7.5, and 10 mmol NaClO per gram of AC to produce TEMPO-oxidized ACs (TACs) that were then mechanically defibrillated into ACNFs (Table 1). Oxidation reactions of AC4-5-5 were terminated when the pH ceased to decrease and lasted 30–168 min with increasing NaClO

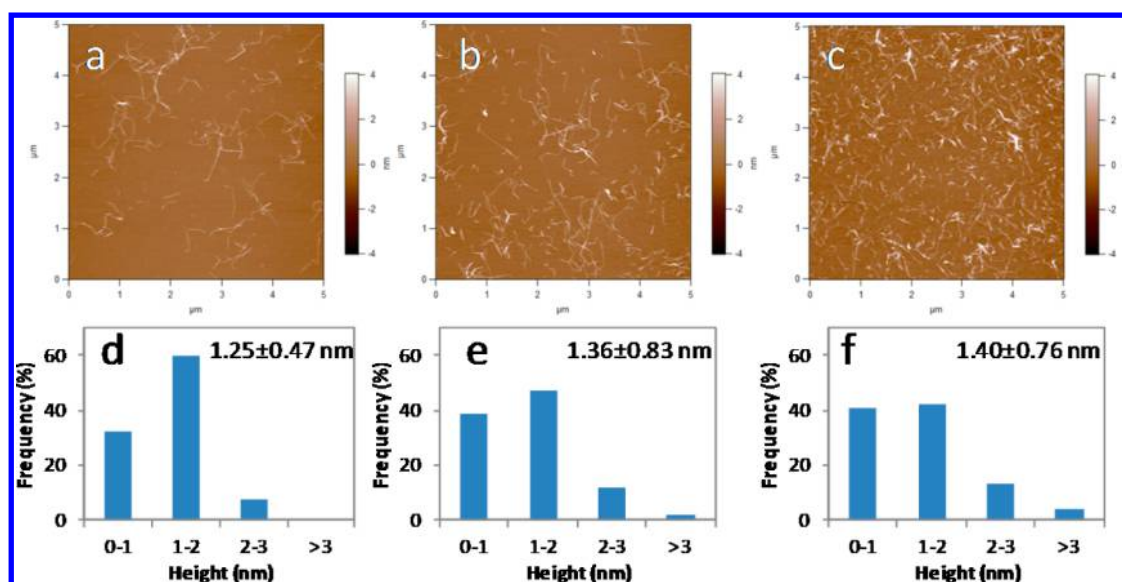


**Figure 2.** AFM images (a–c) and height distribution (d–f) of ACNFs: (a, d) ACNF5, (b, e) ACNF7.5, (c, f) ACNF10.

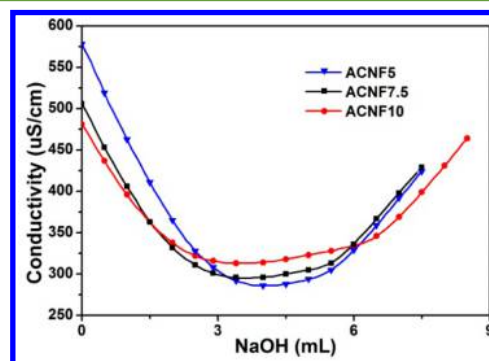
concentrations, yielding 39.7% TAC5, 38.3% TAC7.5, and 31.5% TAC10 at 5, 7.5, and 10 mmol NaClO, respectively. In all three cases, the light yellow ACs turned into pure white TACs, indicating removal and dissolution of residual lignin in AC4-5-5 by TEMPO oxidation. With consideration of the yields of AC4-5-5 (47.6%) and pure cellulose (35.5%), these TAC yields suggest that most noncellulosics were removed upon oxidation with 5 and 7.5 mmol NaClO whereas some amorphous cellulose may be lost at the highest 10 mmol NaClO level. Mechanical blending of TACs for 30 min yielded 34.2% ACNF5, 36.5% ACNF7.5, and 30.2% ACNF10, representing 86.1%, 95.3%, and 95.9% conversion, showing optimal conversion (95.3%) and yield (36.5%) at 7.5 mmol of NaClO.

The yield of ACNFs produced from alkali treatment was compared with those of CNF from pure cellulose and HCNF from holocellulose, all from rice straw (Table 1).<sup>17,18</sup> Cellulose was isolated by three-step toluene/ethanol extraction, acidified NaClO<sub>2</sub> oxidation of lignin, and KOH dissolution of hemicellulose as mentioned before. Holocellulose was produced by omitting the third alkali dissolution step. At the same 5 mmol NaClO level,<sup>17,18</sup> TEMPO-mediated oxidation of holocellulose and cellulose yielded 37.9% THCS and 30.8% TCS, respectively. After mechanical blending, 88.9% and 94.5% of the respective THCS and TCS were converted to HCNF5 and CNF5. The lower conversion rates for ACNF and HCNF were consistent with less oxidant available for oxidizing cellulose after removing the noncellulosics. The 33.7% and 29.1% yields of the respective HCNF5 and CNF5 were 2.8% and 7.4% lower than the 36.5% yield of ACNF7.5 (Table 1).

**Sizes and Surface Carboxyl Content of ACNFs.** The average thickness of ACNFs from AFM height profiles was 1.25 ( $\pm 0.47$ ), 1.36 ( $\pm 0.83$ ), and 1.40 ( $\pm 0.76$ ) nm for ACNF5, ACNF7.5, and ACNF10, respectively (Figure 2 and Table 1). While the average ACNF thickness showed no statistical difference ( $p < 0.05$ ), more numerous ACNFs that were thinner than 1 nm thick were observed with increasing NaClO concentrations. ACNF lengths also shortened with increasing oxidant levels. ACNF5 was hundreds of nanometers to about 1  $\mu\text{m}$  long whereas ACNF7.5 had some 100–300 nm long nanofibrils and ACNF10 contained even more 100–200 nm

long nanofibrils. At the lower 5 mmol NaClO level, most of the remaining lignin and hemicelluloses in AC4-5-5 were removed by oxidation, while the extra agent at 10 mmol of NaClO reacted with amorphous cellulose and crystalline surfaces. At the 10 mM NaClO level, more extensive oxidation of amorphous cellulose may have occurred, leading to depolymerization of cellulose chains and loss of cellulose fragments to shorter ACNF10 lengths. The cellulose nanofibril thicknesses from the same coupled TEMPO oxidation-blending of differently pretreated rice straw materials were also similar, i.e., 1.25 ( $\pm 0.47$ ), 1.36 ( $\pm 0.62$ ), and 1.55 ( $\pm 0.54$ ) nm for ACNF5, HCNF5, and CNF5, respectively (Table 1).<sup>17</sup> CNF5 contained some shorter (100–300 nm long) nanofibrils, while most HCNF5 and ACNF5 species were longer than 500 nm, again indicating the presence of hemicelluloses and/or lignin consumed oxidant agents but possibly having lessened effects on cellulose chain scissions.

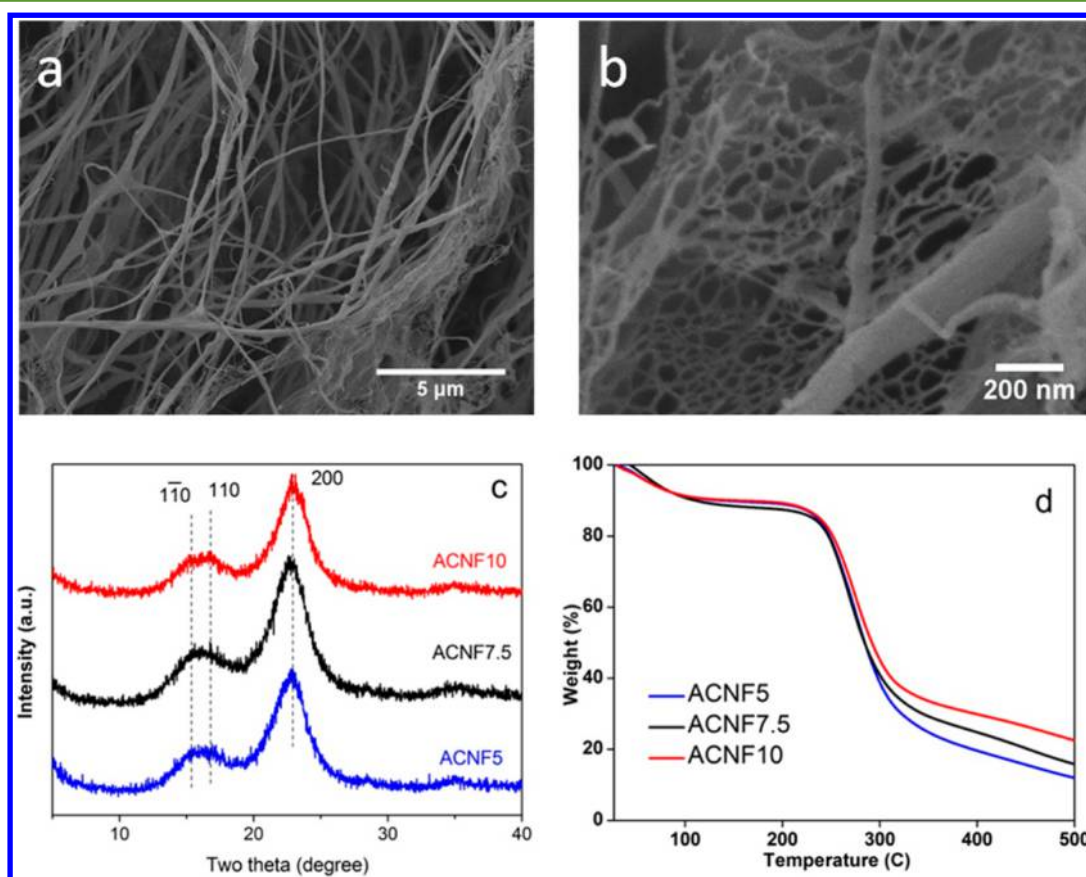
The surface carboxyl contents of ACNFs were measured by conductometric titrations whose curves showed parabolic-shape relationships with NaOH volume for all three ACNFs (Figure 3). TEMPO oxidation converts the C6 hydroxyls to carboxyls (COOH) which, upon reacting with NaOH at pH 10, form carboxylates (COO<sup>-</sup>Na<sup>+</sup>). At the onset of titration, the added HCl converts COO<sup>-</sup> to COOH. While titrating with NaOH, the conductivity decreases initially from neutralizing excess



**Figure 3.** Conductometric titration curves of ACNF5, ACNF7.5, and ACNF10.

**Table 2.** Yield and Compositions of Dewaxed Rice Straw (RS), AC4-5-5, Holocellulose, Cellulose, TAC5, THC5, and TCS<sup>a</sup>

	dewaxed rice straw	AC4-5-5	holo cellulose	cellulose	TAC5	THC5	TCS
yield (% RS)	94.4	47.6	72.8	35.5	39.7	38.3	31.5
			Composition (% Mass)				
neutral sugar	53.2	89.8	64.8	94.4	68.9	54.3	61.0
glucose	32.8	71.7	40.5	79.1	60.3	47.2	53.0
xylose	15.9	13.3	19.0	13.1	8.6	7.1	8.0
arabinose	3.0	3.3	3.9	1.8	ND	ND	ND
galactose	1.4	1.4	1.4	0.4	ND	ND	ND
Klason lignin	11.9	5.1	4.4	4.9	3.4	10.2	7.9
ash	17.2	6.3	20.2	3.3	4.8	6.9	3.3
unassigned	17.8		10.6		22.9	28.6	27.9

<sup>a</sup>ND: not detected.**Figure 4.** Freezing induced self-assembled cellulose structures: SEM images of fibers assembled from ACNF5 at 0.1% (a) 5000X, (b) 50000X, (c) X-ray diffractograms, and (d) TGA thermograms.

HCl, then reaches a plateau in neutralizing the weak carboxylic acid on the ACNFs, and finally increases sharply from the excess NaOH. The total COOH and COO<sup>-</sup> carboxyl content of ACNFs was calculated from NaOH added in the plateau regions to be 0.96, 1.25, and 1.62 mmol per g of ACNF (Table 1), or 0.16, 0.20, and 0.26 mol per mol of anhydroglucose (AG) for ACNF5, ACNF7.5, and ACNF10, respectively. At the same 5 mmol NaClO level, CNF5 and HCNF5 contained 1.36 and 1.09 mmol/g COOH/COO<sup>-</sup> groups, respectively, and both are higher than the 0.96 mmol/g of ACNF5 (Table 1). Further increasing NaClO concentration to 7.5 mmol resulted in ACNF7.5 of total COOH and COO<sup>-</sup> carboxyl content comparable to that of CNF5. In short, ACNFs produced from less purified cellulose exhibited similar thickness, but

longer fibril length, lower surface carboxyl content, and higher yield than those from pure cellulose.

**Compositional Analysis of Rice Straw Fibers and Their TEMPO-Oxidized Products.** To further understand the essential difference among ACNFs, CNFs, and HCNFs, the chemical compositions of their precursors were analyzed (Table 2). From dewaxed rice straw, the double alkali pretreatment was impressively effective in removing approximately 80% Klason lignin, 80% ash, and more than half of the nonglucose sugars (i.e., hemicelluloses). Sodium chlorite bleaching of dewaxed rice straw generated holocellulose that contained slightly less lignin as expected, but had little effect on the silica ash. Compared to cellulose from a three-step toluene/ethanol–NaClO<sub>2</sub>–KOH process, which contained 79.1% glucose, AC4-5-5 contained slightly less cellulose, but higher hemicelluloses,

Table 3. Properties of Self-Assembled Nanofibrils<sup>a</sup>

nanofibrils	fiber width (nm)	Si (wt %)	CrI (%)	cryst size (200 plane, nm)	original surface primary C6 hydroxyl (per AG)	surface primary hydroxyl-to-carboxyl convert (%)	$T_{\max}$ (°C)	char at 500 °C (%)
ACNF5	197 ± 79/ 12 ± 3	0.20	68	2.7	0.24	65	274	12.0
ACNF7.5	ND	0	68	2.7	0.25	80	271	15.8
ACNF10	ND	ND	70	3.0	0.23	115	270	22.5
CNF5	497 ± 161	0	69	2.6	0.26	85	263	24.4
HCNF5	94 ± 33	0.56	68	2.6	0.26	69	274	27.8

<sup>a</sup>Except for silicon contents, data on CNF5 and HCNF5 were from previous studies.<sup>17,18</sup> ND: not determined.

ash, and slightly higher lignin. It should be noted that the three-step standard process did not produce 100% pure cellulose as indicated by the neutral sugar analysis, but this most purified product was referred as rice straw “cellulose” hereafter for consistency. Alkali treatment could not dissolve hemicelluloses entrapped within or between cellulose microfibrils.<sup>23</sup> Among different hemicelluloses, xylans were among the most resilient to alkalis perhaps due to their strong hydrogen bonding and hydrophobic interaction with cellulose.<sup>24</sup> In a similar study, xylans were found to be present in bleached eucalyptus pulp when treated with 0.5–2 M NaOH.<sup>25</sup>

At the same 5 mmol NaClO level, TEMPO-mediated oxidation of AC4-5-5, holocellulose, and cellulose yielded the highest neutral sugars at 68.9% from TAC5, followed by 61.0% from TC5 and 54.5% from THCS, whereas the proportion of glucose out of neutral sugars was only slightly higher for TAC5 (87.5%) than for THCS and TC5, both at 86.9%. The absence of arabinose and galactose in all indicated their effective removal by TEMPO oxidation whereas the partial remaining of xylose (i.e., xylan) was probably due to the lack of C6-primary hydroxyl to be oxidized by TEMPO-mediated oxidation.<sup>19</sup> Selective removal of hemicelluloses during TEMPO oxidation was in accordance with what was observed previously.<sup>19,25,26</sup> The Klason lignin content of TAC5 was also lower than that of ACS-4-4 perhaps due to the degradation of the  $\beta$ -O-4 structure of lignin by the oxidation agents.<sup>27</sup> Both the amount of NaClO added and the precursor fiber sizes affect the dissolution of lignin.<sup>27,28</sup> In a comparison to TC5 (3.3%), TAC5 had higher ash content (4.8%), but it was lower than that of the silica containing THCS (6.9%).<sup>17</sup> The unassigned products may include uronic acids and other losses during the measurements. The fewer unassigned components in TAC5 (22.9%) than in TC5 (27.9%) and THCS (28.6%) were consistent with the lower efficiency of hydroxyl-to-carboxyl (e.g., glucose to glucuronic acid) conversion of AC4-5-5 (0.96 mmol/g<sub>ACNF5</sub> or 16.9% glucuronic acid) than either holocellulose (1.09 mmol/g<sub>HCNF5</sub> or 19.1% glucuronic acid) or cellulose (1.36 mmol/g<sub>CNF5</sub> or 23.9% glucuronic acid). TEMPO oxidation at the same 5 mmol NaClO level required less time (30 min) to generate TAC5 from the double alkali treated cellulose AC4-5-5 than from cellulose (71 min) and holocellulose (86 min), but the resulting ACNF5 also contained fewer carboxyl groups than CNF5 and HCNF5.

**Properties of Freeze-Drying Induced Self-Assembled ACNFs.** Rapid freezing 0.1% ACNF5 suspension in liquid nitrogen (−196 °C) followed by freeze-drying generated white fluffy randomly oriented fibrous mass (Figure 4a). Most fibers were 100–300 nm wide and hundreds of micrometers long, with many numerous finer nanofibers in spider net-like structure (Figure 4b). The average fiber diameters of these two populations were 197 (±79) nm and 12 (±3) nm,

respectively (Table 3). Few thicker ribbons of 400–1000 nm width were also observed. During rapid freezing, individual ACNF5 species self-assembled with each other laterally and longitudinally into fibers that were 10–200 times thicker and hundreds of times longer than the individual ACNF5.

Interestingly, most of the fibers self-assembled from ACNF5 averaged 197 nm wide, less than half the width as compared to those from CNF5 (497 ± 161 nm), but twice as thick as those from HCNF5 (94 ± 33 nm), all from exactly the same oxidation conditions (Table 3). The thinner spider net-like structure was not observed in either ACNF5 or CNF5 from the same 0.1% concentration, but similar bimodally sized nanofibrils (164 ± 70 nm and 18 ± 5 nm) were also observed for self-assembled HCNF5 from a much lower 0.01% concentration.<sup>17</sup> The less surface charged ACNF5 assembling into finer fibers was consistent with previous observations that more highly surface oxidized CNFs tended to self-assemble into thicker ultrafine fibers.<sup>18,29</sup> The thinner self-assembled fibers of ACNF5s than those of CNF5s may also be attributed to the interference of the noncellulosics, such as less hydrophilic hemicelluloses and/or silica, in self-assembly. TEMPO oxidation dissolved and removed most of the hemicelluloses except xylan. However, the impact of xylan in ACNF5, CNF5, and HCNF5 may be comparable since the proportion of xylose out of neutral sugars was very similar in TAC5, THCS, and TC5. Silica in HCNF5 (0.56 wt % Si) was thought to have contributed to the much reduced self-assembled fibers as compared to those of silicon-free CNF5.<sup>17</sup> However, the silicon contents in ACNFs were very low, i.e., 0.2 wt % for ACNF5 and 0 for ACNF7.5, and close to the detection limit of EDS, which thus may not be as clearly evident. The FTIR results also confirmed that ACNFs had similar chemical composition to that of CNF5, but not HCNF5 which exhibited Si–O–Si stretching bands of silica.<sup>10,17</sup> In conclusion, at the same freeze-drying conditions, ACNF5 self-assembled to fine fibers, 60% thinner than those of CNF5, but twice as thick as those of HCNF5, the former attributed to the surface charge difference whereas the latter was not as clearly linked to the silicon contents in these nanofibrils.

The freeze-dried ACNFs exhibited cellulose I $\beta$  structure with three main characteristic peaks at  $2\theta = 14.5^\circ$ ,  $16.6^\circ$ , and  $22.7^\circ$   $2\theta$  corresponding to the 1 $\bar{1}0$ , 110, and 200 crystallographic planes as expected (Figure 4c). The ACNF5, ACNF7.5, and ACNF10 exhibited similar crystallinity indexes (CrIs) of 68%, 68%, and 70%, respectively, and similar average crystal sizes of 2.7, 2.7, and 3.0 nm, respectively (Table 3). ACNF5 exhibited similar crystallinity (CrI = 68%) and crystal size (2.7 nm) as those of CNF5 (69%, 2.6 nm) and HCNF5 (68%, 2.6 nm). On the basis of the crystalline dimensions, surface primary C6 hydroxyls were calculated to be 0.24, 0.25, and 0.23 per anhydroglucose (AG) in the original ACNF5, ACNF7.5, and

ACNF10, respectively (Table 3). Assuming all oxidation occurred in the crystalline surfaces, the extent to which the surface primary hydroxyls was converted to COOH/COO<sup>-</sup> groups was 65%, 80%, and 115% for ACNF5, ACNF7.5, and ACNF10, respectively, consistent with increasing levels of oxidation. The 15% over the full possible surface OH/(COOH + COO<sup>-</sup>) conversion on ACNF10 could be due to the oxidation of some ACNF10 surface glucan chains to homopolyglucuronic acid.<sup>30</sup> The 65% surface primary carboxyl conversion of ACNF5 was lower than that of CNF5 (85%) and HCNF5 (69%), likely due to the consumption of oxidant in oxidizing lignin.

The TGA curves of all ACNFs showed less than 10% initial mass loss around 100 °C from evaporation of adsorbed water, followed by rapid mass losses in 250–300 °C from decomposition and finally slow mass loss during charring (Figure 4d). The temperature in which most cellulose decomposed ( $T_{\max}$ ) decreased slightly from 274 to 271 °C and 270 °C while the char residues at 500 °C increased from 12.0% to 15.8% and 22.5% for ACNF5, ACNF7.5, and ACNF10, respectively, consistent with the decreased thermal stability and higher chars with increasing carboxylate contents previously reported.<sup>18</sup> ACNFs were slightly more thermally stable than CNF5 and similar to HCNF5, but had 50.8% and 56.8% less chars than CNF5 and HCNF5, respectively (Table 3), perhaps due to less well self-assembled structures from the less carboxylated surfaces to hydrogen bonds<sup>18</sup> and the lower silicon content.

## CONCLUSIONS

Alkaline cellulose nanofibrils (ACNFs) have been efficiently isolated from rice straw by streamlined alkali pretreatment followed by TEMPO-mediated oxidation followed by mechanical blending. Most hemicelluloses and lignin in rice straw were shown to be readily dissolved whereas silica was completely removed in two repetitive alkali treatment (4% NaOH, 70 °C, 5 min), yielding 47.6% cellulose-rich solid or alkaline cellulose. Optimal TEMPO oxidation with 7.5 mmol NaClO per g of cellulose and 30 min mechanical blending produced 38.3% TEMPO-oxidized alkaline cellulose (TAC) and 36.5% ACNFs, respectively, higher than 29.1% of cellulose nanofibrils (CNFs) produced from rice straw cellulose isolated by a three-step dewaxing–sodium chlorite oxidation–alkali leaching process and 33.7% of holocellulose nanofibrils (HCNFs) by the same process without the alkali step. The ACNF7.5 species were 1.36 (±0.83) nm thick and 100–300 nm long and contained 1.25 mmol carboxylate per gram of cellulose. Derived at the 5 mmol NaClO level, ACNF5 exhibited similar chemical composition, thickness (1.25 nm), and crystallinity (68% CrI) as those of CNF5 (1.55 nm, 69%) and HCNF5 (1.36 nm, 68%), but longer than CNF and less surface charge (0.96 mmol/g) than CNF (1.36 mmol/g) and HCNF (1.09 mmol/g). Upon rapid freezing of 0.1% suspensions at −196 °C, ACNFs self-assembled to bimodally sized fibers (197 and 12 nm), with some thicker than those from HCNFs (94 nm), but much thinner than those from CNF (497 nm). The double alkali pretreatment (4% NaOH, 70 °C, 5 min) of dewaxed rice straw has been shown to be highly effective in removing most noncelluloses and generating more of the less charged but longer ACNFs that self-assembled to a lesser extent than CNF5 from the most purified cellulose. While the purity of cellulose precursors had little effect on the nanofibril thickness and crystallinity, the presence of noncelluloses lessened the effects

on surface oxidation and fibril lengths, resulting in distinctly different self-assembled structures upon freezing and freeze-drying. Findings from this study offer further pretreatment choices in purifying cellulose for generating cellulose nanofibrils that present additional attributes for more diverse applications.

## AUTHOR INFORMATION

### Corresponding Author

\*Phone: +1 530 752 0843. E-mail: ylhsieh@ucdavis.edu.

### ORCID

You-Lo Hsieh: 0000-0003-4795-260X

### Notes

The authors declare no competing financial interest.

## ACKNOWLEDGMENTS

Financial support for this research from USDA NIFA (2011-67021-20034), California Rice Research Board (RU-9), Guangdong-Hong Kong joint innovation project (2014B050505019), and President Foundation of South China Agricultural University (South China University of Technology) is greatly appreciated. The authors are grateful to Ying Shen, Dr. Jiang Feng, and Dr. Sixiao Hu for assistance with rice straw alkali treatments. We also acknowledge Dr. Hao Liu and Jianliang Sun at SCAU for their help with HPAEC sample preparations.

## REFERENCES

- (1) Eichhorn, S. J.; Dufresne, A.; Aranguren, M.; Marcovich, N. E.; Capadona, J. R.; Rowan, S. J.; Weder, C.; Thielemans, W.; Roman, M.; Renneckar, S.; Gindl, W.; Veigel, S.; Keckes, J.; Yano, H.; Abe, K.; Nogi, M.; Nakagaito, A. N.; Mangalam, A.; Simonsen, J.; Benight, A. S.; Bismarck, A.; Berglund, L. A.; Peijs, T. Review: current international research into cellulose nanofibres and nanocomposites. *J. Mater. Sci.* **2010**, *45*, 1–33.
- (2) Moon, R. J.; Martini, A.; Nairn, J.; Simonsen, J.; Youngblood, J. Cellulose nanomaterials review: structure, properties and nanocomposites. *Chem. Soc. Rev.* **2011**, *40*, 3941–3994.
- (3) García, A.; Gandini, A.; Labidi, J.; Belgacem, N.; Bras, J. Industrial and crop wastes: A new source for nanocellulose biorefinery. *Ind. Crops Prod.* **2016**, *93*, 26–38.
- (4) Rodríguez, A.; Moral, A.; Serrano, L.; Labidi, J.; Jiménez, L. Rice straw pulp obtained by using various methods. *Bioresour. Technol.* **2008**, *99*, 2881–2886.
- (5) Jackson, M. G. Review article: The alkali treatment of straws. *Anim. Feed Sci. Technol.* **1977**, *2*, 105–130.
- (6) Xiao, B.; Sun, X. F.; Sun, R. Chemical, structural, and thermal characterizations of alkali-soluble lignins and hemicelluloses, and cellulose from maize stems, rye straw, and rice straw. *Polym. Degrad. Stab.* **2001**, *74*, 307–319.
- (7) Siro, I.; Plackett, D. Microfibrillated cellulose and new nanocomposite materials: a review. *Cellulose* **2010**, *17*, 459–494.
- (8) Dutta, S.; De, S.; Saha, B.; Alam, M. I. Advances in conversion of hemicellulosic biomass to furfural and upgrading to biofuels. *Catal. Sci. Technol.* **2012**, *2*, 2025–2036.
- (9) Hansen, C. M.; Bjorkman, A. The ultrastructure of wood from a solubility parameter point of view. *Holzforschung* **1998**, *52*, 335–344.
- (10) Hu, S.; Gu, J.; Jiang, F.; Hsieh, Y.-L. Holistic rice straw nanocellulose and hemicelluloses/lignin composite Films. *ACS Sustainable Chem. Eng.* **2016**, *4*, 728–737.
- (11) Mikkonen, K. Recent studies on hemicellulose-based blends, composites and nanocomposites. In *Advances in Natural Polymers*; Thomas, S., Visakh, P. M., Mathew, A. P., Eds.; Springer: Berlin, 2013; Chapter 9, pp 313–336.



- (12) Suhas; Carrott, P. J. M.; Ribeiro Carrott, M. M. L. Lignin – from natural adsorbent to activated carbon: A review. *Bioresour. Technol.* **2007**, *98*, 2301–2312.
- (13) Reddy, N.; Yang, Y. Biofibers from agricultural byproducts for industrial applications. *Trends Biotechnol.* **2005**, *23*, 22–27.
- (14) Lu, P.; Hsieh, Y. L. Preparation and characterization of cellulose nanocrystals from rice straw. *Carbohydr. Polym.* **2012**, *87*, 564–573.
- (15) Jiang, F.; Hsieh, Y.-L. Holocellulose nanocrystals: amphiphilicity, oil/water emulsion, and self-assembly. *Biomacromolecules* **2015**, *16*, 1433–1441.
- (16) Jiang, F.; Hsieh, Y. L. Chemically and mechanically isolated nanocellulose and their self-assembled structures. *Carbohydr. Polym.* **2013**, *95*, 32–40.
- (17) Gu, J.; Hsieh, Y.-L. Surface and structure characteristics, self-Assembling, and solvent compatibility of holocellulose nanofibrils. *ACS Appl. Mater. Interfaces* **2015**, *7*, 4192–4201.
- (18) Jiang, F.; Han, S.; Hsieh, Y.-L. Controlled defibrillation of rice straw cellulose and self-assembly of cellulose nanofibrils into highly crystalline fibrous materials. *RSC Adv.* **2013**, *3*, 12366–12375.
- (19) Kuramae, R.; Saito, T.; Isogai, A. TEMPO-oxidized cellulose nanofibrils prepared from various plant holocelluloses. *React. Funct. Polym.* **2014**, *85*, 126–133.
- (20) Nasri-Nasrabadi, B.; Behzad, T.; Bagheri, R. Extraction and characterization of rice straw cellulose nanofibers by an optimized chemomechanical method. *J. Appl. Polym. Sci.* **2014**, *131*, 2113–2124.
- (21) Jiang, F.; Kondo, T.; Hsieh, Y.-L. Rice straw cellulose nanofibrils via aqueous counter collision and differential centrifugation and their self-assembled structures. *ACS Sustainable Chem. Eng.* **2016**, *4*, 1697–1706.
- (22) Chaker, A.; Alila, S.; Mutjé, P.; Vilar, M.; Boufi, S. Key role of the hemicellulose content and the cell morphology on the nanofibrillation effectiveness of cellulose pulps. *Cellulose* **2013**, *20*, 2863–2875.
- (23) Pauly, M.; Albersheim, P.; Darvill, A.; York, W. S. Molecular domains of the cellulose/xyloglucan network in the cell walls of higher plants. *Plant J.* **1999**, *20*, 629–39.
- (24) Mazeau, K.; Charlier, L. The molecular basis of the adsorption of xylans on cellulose surface. *Cellulose* **2012**, *19*, 337–349.
- (25) Meng, Q.; Li, H.; Fu, S.; Lucia, L. A. The non-trivial role of native xylans on the preparation of TEMPO-oxidized cellulose nanofibrils. *React. Funct. Polym.* **2014**, *85*, 142–150.
- (26) Sbiai, A.; Kaddami, H.; Sautereau, H.; Maazouz, A.; Fleury, E. TEMPO-mediated oxidation of lignocellulosic fibers from date palm leaves. *Carbohydr. Polym.* **2011**, *86*, 1445–1450.
- (27) Ma, P.; Fu, S.; Zhai, H.; Law, K.; Daneault, C. Influence of TEMPO-mediated oxidation on the lignin of thermomechanical pulp. *Bioresour. Technol.* **2012**, *118*, 607–610.
- (28) Okita, Y.; Saito, T.; Isogai, A. TEMPO-mediated oxidation of softwood thermomechanical pulp. *Holzforschung* **2009**, *63*, 529–535.
- (29) Jiang, F.; Hsieh, Y.-L. Self-assembling of TEMPO oxidized cellulose nanofibrils as affected by protonation of surface carboxyls and drying methods. *ACS Sustainable Chem. Eng.* **2016**, *4*, 1041–1049.
- (30) Hirota, M.; Furihata, K.; Saito, T.; Kawada, T.; Isogai, A. Glucose/glucuronic acid alternating co-polysaccharides prepared from TEMPO-oxidized native celluloses by surface peeling. *Angew. Chem., Int. Ed.* **2010**, *49*, 7670–7672.